CHAPTER 5

High Pressure Raman Spectroscopic Study on Chirality inducing Agent: A Case Study of Sodium Dithionite ($Na_2S_2O_4$)

Abstract

The most widely used reducing agent, Sodium dithionite ($Na_2S_2O_4$), has very long S-S bond (2.389Å). It has two short S-O bonds in eclipsed configuration and are attached side by side to the long S-S bond (main bar). In aqueous solution, it exists in equilibrium as [$SO_2^{-\cdot}$] radical state due to easy cleavage of its long S-S . Its structure is similar to the compound sodium dithionate ($Na_2S_2O_6$) that is used in reactions to induce chirality. In this chapter, we have reported our experiments indicating that $Na_2S_2O_4$ also can impart chirality to the oxidized products. Observing long S-S bond, the symmetry of SO bonds with respect to the molecule undergoing chiral formation and its chirality inducing property motivated us to investigate the solid-state behaviour of $Na_2S_2O_4$ under quasi-hydrostatic (up to 34.5 GPa) and non-hydrostatic (30.2 GPa) pressure environments using diamond anvil cell and by Raman spectroscopy. To investigate in detail, solid state synthesis reactions of $Na_2S_2O_4$ with acetophenone and benzil respectively were carried out under high pressure, in anticipation of chiral product formation. In both pressure environments, main vibrational modes blue shifted with increase in pressure and some changes in dω/dP were observed. S-S Stretching bond and stretching of S-O bonds were observed to be related to each other. It's interesting to note that the pressure values of ~ 0.3 GPa, ~ 3.2 GPa, ~ 7.8 GPa, and ~ 18.7 GPa at which we observed changes in the Raman spectra of $Na_2S_2O_4$ were similar to the pressure values that were observed in literature in high pressure studies of SO_2. During compression above 7.8 GPa, a new S-S-bond was developed at a high frequency side of 261 cm^{-1} under quasi-hydrostatic as well as in non-hydrostatic pressure environments. Changes in the S-S-bond and other modes were completely reversible on decompression. The findings of this work are significant and can help to understand the reactivity of disulphide bridged systems, particularly proteins, when they are under external stress.

5.1 Introduction

Sodium dithionite ($Na_2S_2O_4$) is a strong reducing and bleaching agent that is used extensively in a variety of sectors, including the textile, paper, and food industries. It is also used in the

reduction of aldehydes and ketones. (Vries & Kellogg, 1980) It is an environmentally hazardous and toxic chemical. (Carter, 1996; Westbroek et al., 1999; J. B. Zhang et al., 2014) It is harmful to the human respiratory system and eyes, (Yan & He, 2008). Its azo based fluorescent probe detection technique reported in the literature can be helpful to detect their toxicity. (Dong et al., 2019)

Sodium dithionite ($Na_2S_2O_4$) has an exceptionally long S-S bond (2.389 Å) which makes it a fascinating molecule to study. (Dunitz, 1956) Some other compounds similar to sodium dithionite ($Na_2S_2O_4$) are $Na_2S_2O_5$ and $Na_2S_2O_6$ with the S-S bond lengths of 2.210 Å and 2.150 Å, respectively. (Takahashi et al., 1982) However, the S-S bond length for ZnS_2O_4 is very long equal to 2.386 Å (Kiers & Vos, 1978) and the normal disulphide bond length is 2.080 Å. (Knop et al., 1988) (9) The SO_2 units are free to rotate because of the long S-S bond and, due to it, the molecule forms the eclipsed conformation in the solid state and staggered conformation in the liquid state. During EPR measurements, aqueous solution showed the presence of the paramagnetic $[SO_2]^{-\cdot}$ radical in equilibrium with $[S_2O_4]^{2-}$.(Rinker et al., 1959) Interestingly, similar to that in the liquid state, early research on $Na_2S_2O_4$ in the solid state also revealed a weak paramagnetic character, indicating the presence of the $[SO_2]^{-\cdot}$radical.(Hodgson et al., 1956) even though a comprehensive EPR investigation and chemical analysis, did not rule out the possibility of even mixed anhydride form $[OSOSO_2]^{2-}$.

The mixed anhydride form $[OSOSO_2]^{2-}$ indicates a path for the non-symmetrical cleavage of two SO_2 units. Thus, all dynamic movements in dithionite ions, comprising S-S bond stretching and other SO_2-related modes including scissor, wagging and twist motion, as well as symmetric and asymmetric stretching motion, require systematic monitoring to understand the behaviour of long S-S bonds. As all of these vibrational modes are Raman active, we attempted to observe and investigate the dynamics of all of the aforementioned vibrational modes under quasi-hydrostatic and non-hydrostatic stress using Raman spectroscopy.

Formation and cleavage of these disulfide bonds and their reversibly reducing and re-oxidizing nature are some of their characteristic properties. (Feige, Matthias J. Braakman, Ineke and Hendershot, 2018; Ling et al., 2020; Manteca et al., 2017; Passam & Chiu, 2019) It has been extensively used by nature to execute several metabolic pathways and regulate gene expression, in addition to controlling the tertiary structure of proteins. Several researchers have investigated the function of mechanical force to investigate the cleavage ability of disulfide bonds. (Aktah & Frank, 2002; Wiita et al., 2006)According to the theory predicted, the change in the S-S bond

length and conformational environment are responsible for the biomolecular chemical reaction, and single-molecule force-clamp spectroscopy provided excellent confirmation for these predictions,(Iozzi et al., 2011; Manyes et al., 2009) thereby emphasizing mechanochemistry. (Do & Friscic, 2017; Neill & Boulatov, 2021; Wiedemann et al., 2020)

Dunitz et al. performed X-ray diffraction studies on sodium dithionite ($Na_2S_2O_4$), which crystallizes in monoclinic form with a = 6.404 ±0.005Å, b = 6.559 ±0.003 Å, c = 6.586 ± .006 Å and β = 119.5° with space group *P*2/*c*, (Dunitz, 1956). Takahashi et al. performed a Raman spectroscopic study on $Na_2S_2O_4$ in crystalline and aqueous state.(Takahashi et al., 1982) Raman spectral analysis shows that the Dithionite ion exists in an eclipsed configuration (C_{2v} symmetry) in the crystalline state and in a staggered configuration (C_{2h} symmetry) in the aqueous state. (Peter & Meyer, 1982; Takahashi et al., 1982) S-S bond lengths are observed to shorten from 2.389 Å (crystalline state) to 2.20-2.26 Å in aqueous state due to decrease in lone pair electrostatic repulsions. Leszczynski et al.(Leszczynski & Zerner, 1989) performed quantum chemical calculations and validated two configurations of $Na_2S_2O_4$ C_{2v} symmetry for the crystalline state and C_{2h} symmetry for the aqueous state.

Additionally, according to the literature, other different configurations of dithionite ion are also possible, including eclipsed, staggered, perpendicular, and planar. (Leszczynski & Zerner, 1989; Takahashi et al., 1982) Tetra ethyl ammonium dithionite exhibits the gauche conformation of the dithionite ion in crystalline form. (Hodgeman et al., 1991) The dithionite ion in ZnS_2O_4. pyridine complex (Kiers & Vos, 1978) and Tin(II) dithionite (Magnusson & Johansson, 1982) $Sn_2(S_2O_4)_2$ has a long S-S bond length of 2.386 Å and 2.350 Å which are comparable to $Na_2S_2O_4$ and both exist in eclipsed geometry. As the S-S bond length increases, the stretching force constant K(S-S) gradually decreases of $S_2O_x^{2-}$.(Takahashi et al., 1982)(As repulsive force constant F(S-S-O) decreases as (S...O) distance increases.(Takahashi et al., 1982; Weinrach et al., 1992)

Vegunta et al.(Vegunta, 2016) performed ATR-FTIR Spectroscopy on $Na_2S_2O_4$ solution to study thermal and chemical stability under anaerobic conditions with respect to pH, temperature, heating time, and concentration. It was found that with an increase in these parameters, the thermal and alkali stability of $Na_2S_2O_4$ solution decreased and it was more stable at pH 11.5 to pH 13. Sodium dithionite decomposes in the presence of air and with time different decomposition products are formed. James et al. (2014) published their work on the decomposition of ten different aged crystalline $Na_2S_2O_4$ samples spanning over 50 years of

shelf life, which were analyzed by iodometric titration, ion chromatography, and Raman Spectroscopy. Their work suggested that the dithionite content in the sample decreases as the sample ages and different decomposition products like sulphite (SO_3^{2-}), sulfate (SO_4^{2-}), thiosulfate ($S_2O_3^{2-}$) , metabisulphite ($S_2O_5^{2-}$) and tetrathionate ($S_4O_6^{2-}$) are formed, which presented significantly different Raman spectra for different aged samples. Their work also pointed out that the maximum decomposition of sodium dithionite takes place in the first month. (James et al., 2015) Additionally, the highest purity of this compound available commercially is not more than 85% which again becomes a challenge to study its behaviour.

Chapter 5 reports the experimental details, the findings from the high-pressure Raman spectroscopic study on the chirality inducing agent Sodium Dithionite ($Na_2S_2O_4$) in quasi-hydrostatic and non-hydrostatic pressure environments and focuses on the questions: how does pressure affect the vibration associated with S-S stretching? Are changes in S-O stretching vibrations correlated to changes in S-S stretching vibrations? For any of these modes, does $d\omega/dP$ show changes? Along with the S-S stretching and S-O stretching modes, the discussion also examines the pressure-induced changes in other modes, such as the SO_2 twist, scissor, and wag modes.

5.2 Materials and Methods

In-situ high pressure Raman spectroscopic experiments were performed on 85% pure $Na_2S_2O_4$ that was purchased from Thermo Fisher Scientific (CAS number :7775-14-6). It was used for the experiment without any additional purification. The sample was stored in a tightly packed vial with proper nitrogen purging under totally anaerobic circumstances. It was kept in a vacuum desiccator. The ketones used in the present work are 1-phenylethanone (acetophenone/ methyl phenyl ketone) purchased from SDFCL (CAS number : 98-86-2) and 1,2-diphenylethane-1,2-dione (benzil) purchased from Merck (CAS number : 134-81-6).

High pressure experiments were performed on a Syntek symmetric DAC diamond anvil cell with Type I diamonds, with a culet size of 400 microns. The sample for the experiment was contained in a stainless-steel gasket (T301) of preindented thickness of 40 microns with a centrally drilled hole of size ~ 130 microns. In order to generate a quasi-hydrostatic pressure environment, silicone oil of 100 cst was used to generate quasi hydro static environment and to generate a non-hydrostatic pressure environment, the sample was filled within the sample cavity with no surrounding media.

A single-frequency Oxxius laser operating at 532 nm was used as an excitation source. A spectrometer model SR-500i-A-R with 1800 lines/mm grating was used to record the Raman spectra attached to the thermoelectrically cooled Andor iDUS charge coupled device camera.

In order to monitor pressure, fine ruby powder was used, and the R1 ruby fluorescence line was used for calibration purposes. (Mao et al., 1986) Within the gasket cavity, chunks of fine ruby powder were placed at three locations. Pressure was measured by averaging the pressure readings from three locations. The R1 and R2 distinct ruby peaks were observed under a non-hydrostatic maximum pressure of 30.2 GPa. In our experiments we observed 1.97 cm^{-1}shift is equivalent to 54 kbar pressure difference. Ruby calibration equation for Quasi-hydrostatic and non-hydrostatic environment.(Mao et al., 1986)

$$\boldsymbol{P = \frac{A}{B}\left\{\left[1 + \left(\frac{\Delta\lambda}{\lambda_0}\right)\right]^{B} - 1\right\}}$$

This calibration relation calculates high pressures shift of the ruby R1 line, where P is the pressure in megabars, λ is the wavelength of Ruby R line, A = 19.04 Mbar, B =7.665 for Quasi-hydrostatic environment and A = 19.04, B = 5 for non-hydrostatic environment.(Mao et al., 1978)

5.3 Results and Discussions

Chemical structure of sodium dithionite is shown in Figure 5.1. Raman spectrum of crystalline $Na_2S_2O_4$ at ambient conditions is shown in Figure 5.2. The spectrum exhibits significant modes owing to S-S stretching vibrations at 178 cm^{-1} and 261 cm^{-1}, 350 cm^{-1} corresponds to SO_2 twist, 513 cm^{-1} is due to SO_2 wag, 929 cm^{-1}, 1005 cm^{-1} and 1030 cm^{-1} modes corresponds to SO_2 symmetric stretching vibrations and 1054 cm^{-1} and 1072 cm^{-1} corresponds to SO_2 asymmetric stretching vibrations. In addition to these modes, weak modes exist at 134 cm^{-1}, 157 cm^{-1}, 300 cm^{-1}, 448 cm^{-1}, 561 cm^{-1}, 668 cm^{-1}, and 974 cm^{-1}.

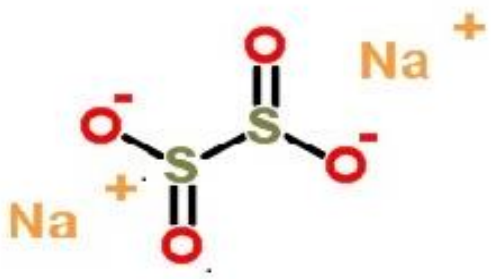

Figure 5.1: Chemical structure of $Na_2S_2O_4$.

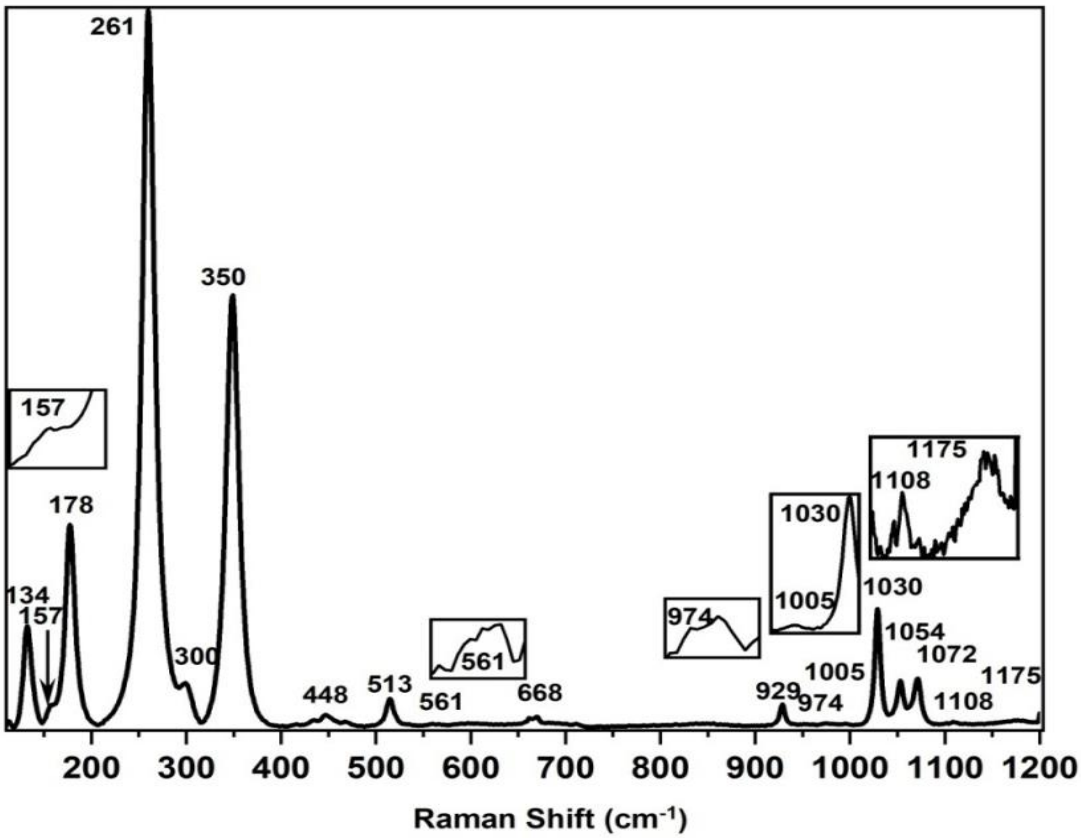

Figure 5.2: Sodium Dithionite's ($Na_2S_2O_4$) ambient Raman spectrum.

It is observed that the addition of Sodium dithionite with ketones breaks the S-S stretching mode and breaks (weakens) the carbonyl bond. It is possible that sodium dithionite imparts chirality to the oxidized product.

Sodium dithionite has a long S-S bond, and it is the most intense peak in the Raman spectrum. We were unable to observe the breaking or weakening of the S-S bond in mortar and pestle, but in the presence of ketones by solid-state mixing (mortar and pestle), it breaks (becomes very weak) instantly, and the carbonyl bond present in ketones also breaks or reduces in

intensity, showing the possibility of sodium dithionite acting as a chirality inducing agent. This indicates that the particular carbon atom attached to ketones may be becoming a prochiral center, indicating the formation of a chiral center.

5.3.1 Vibrational Raman Spectra of Sodium Dithionite in the Presence of Ketones

Chirality induction by $Na_2S_2O_4$: Hypothetical Reaction Scheme

Hypothetical reactions of chirality induction by sodium dithionite ($Na_2S_2O_4$) in the presence of ketones (1-phenylethanone (acetophenone/ methyl phenyl ketone) and 1,2-diphenylethane-1,2-dione (benzil) are shown in Figure. 5.3.

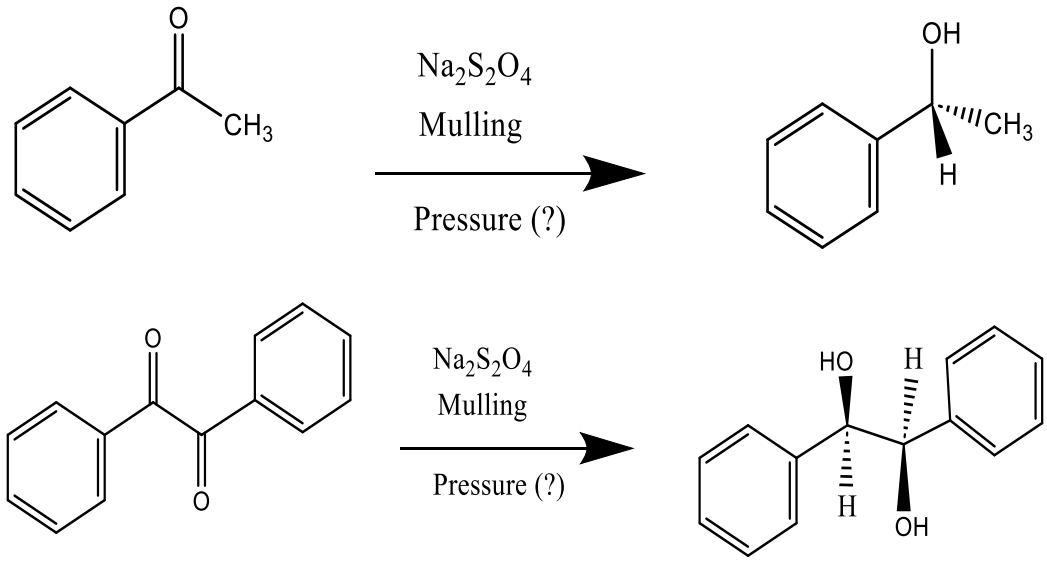

Figure 5.3: Chirality induction by $Na_2S_2O_4$: Hypothetical Reaction Scheme.

The reactions shown in Figure 5.3 indicate that it is possible that the carbon atom attached to the ketone may become a chiral center in the presence of sodium dithionite ($Na_2S_2O_4$), which may act like a chirality inducing agent. To check the chirality inducing properties of $Na_2S_2O_4$, a solid state synthesis reaction between sodium dithionite and ketones was performed in mortar and pestle. The ketones used in the present purpose are 1-phenyl-1-one (acetophenone/ methyl phenyl ketone) and 1,2-diphenylethane-1,2-dione (benzil). The long S-S bond does not break in mortar and pestle, but it breaks (weakens) instantly in the presence of ketones by solid-state mixing (mortar and pestle).

Vibrational Raman spectra of the product were recorded, and they indicated instant weakening (breaking) of the S-S stretching mode in the presence of ketones, as shown in Figures 5.4 and 5.6. Intensity of carbonyl bond vibrational frequency is observed to reduce in intensity which can be observed in Figures 5.5 and 5.6. Addition of a drop of methanol when acetophenone and benzil are used as ketones, makes the carbonyl bond either break or substantially weaken.

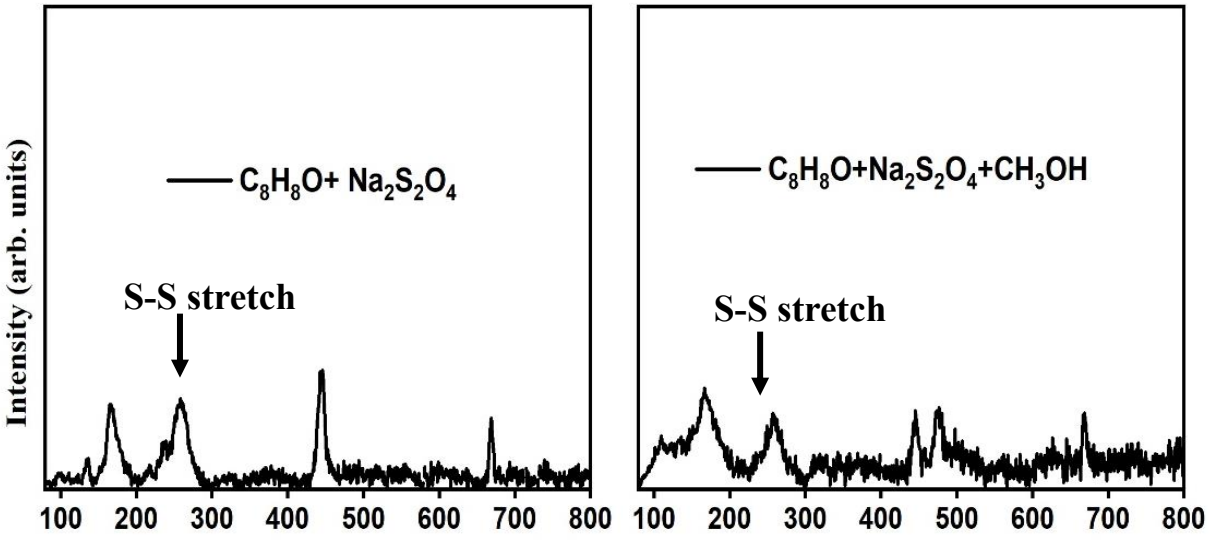

Figure 5.4: Sodium dithionite and acetophenone mixed well in a mortar and pestle instantly weaken the S-S stretching mode. A drop of methanol reduces the intensity of the S-S stretching bond.

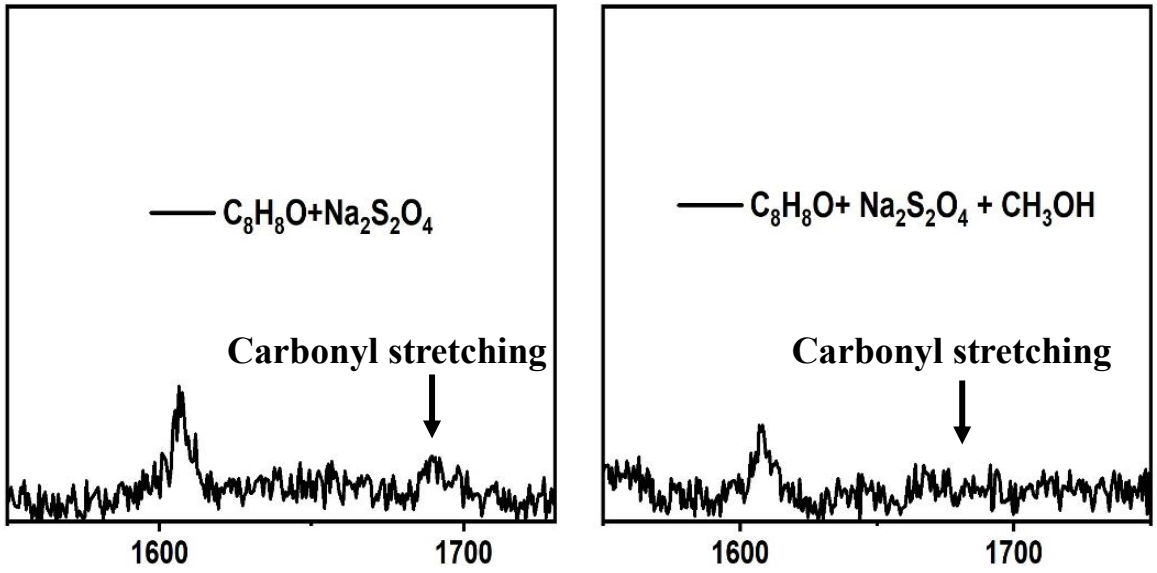

Figure 5.5: Sodium dithionite and acetophenone mixed well in a mortar and pestle instantly weaken the carbonyl bond frequency, and after adding a drop of methanol, break the carbonyl bond completely.

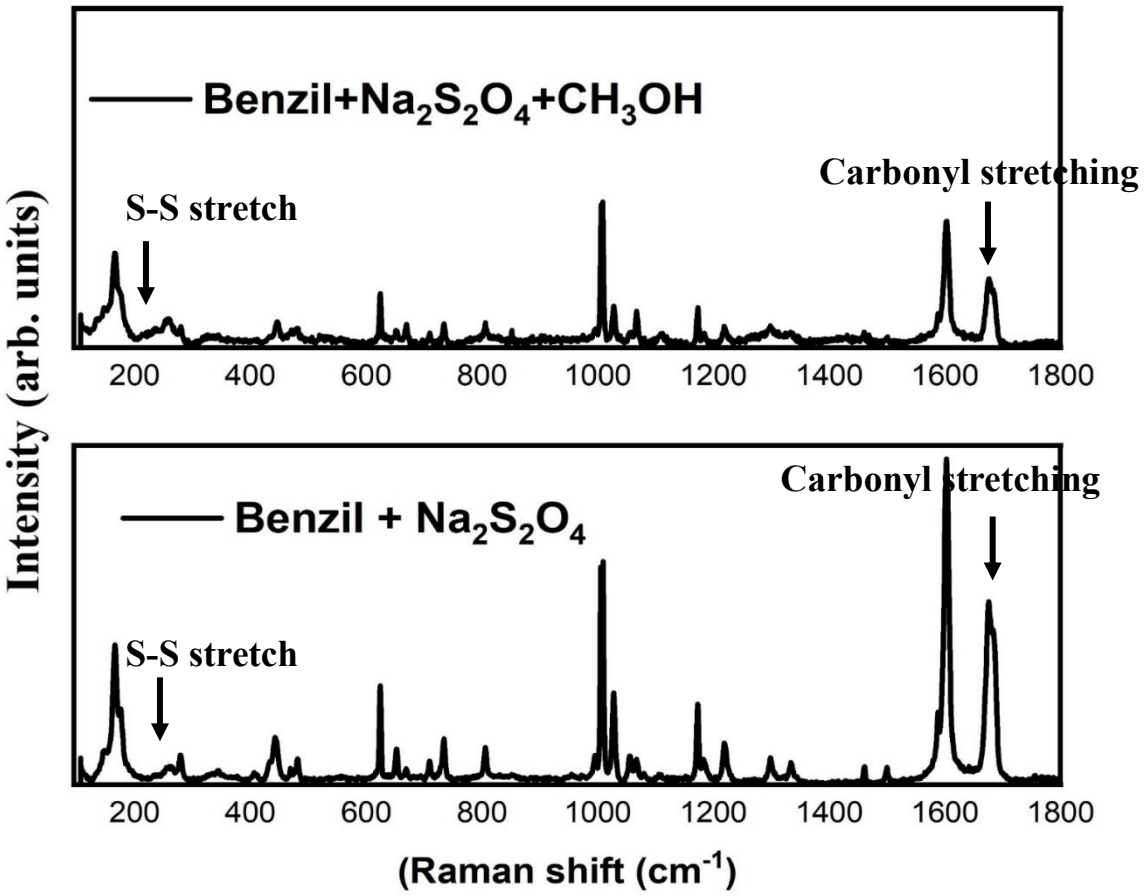

Figure 5.6: Sodium dithionite and benzil are mixed well in a mortar and pestle. It instantly weakens the S-S stretching bond, and after adding a drop of methanol, it weakens the carbonyl bond.

Breaking and intensity reduction of the carbonyl bond in the presence of ketones indicate that a particular carbon atom attached to ketones may be becoming a prochiral center, indicating formation of a chiral center. The goal of our study is to show that sodium dithionite ($Na_2S_2O_4$), similar to sodium dithionate ($Na_2S_2O_6$), which is used in reactions to induce chirality can also act like a chirality inducing agent. As we observed these effects in high pressure solid state synthesis, we further thought to see the dynamics of sodium dithionite molecules under more extreme pressure. These results prompted us to study the dynamics of sodium dithionite under extreme pressure. High pressure effects were investigated in quasi hydrostatic and non-hydrostatic pressure environments.

5.3.2 Raman Modes of Crystalline Sodium Dithionite ($Na_2S_2O_4$)

Raman modes of crystalline Sodium Dithionite ($Na_2S_2O_4$) at ambient conditions are shown in Table 5.1. Observed modes and their corresponding assignments are based on previous reports.

Table 0.1: Raman modes at ambient condition of crystalline Sodium Dithionite ($Na_2S_2O_4$).

(Degen & Newman, 1993; James et al., 2015; Leszczynski & Zerner, 1989; Nims et al., 2019; Rintoul et al., 1997; Takahashi et al., 1982)

Raman Frequency (cm^{-1})	**Assignments**
134	Not known [10]
157	S-S asymmetric bending vibration in Sulphur
178	S-S stretch
261	S-S stretch
300	~ SSO Rock/Twist in Sodium thiosulphate ($Na_2S_2O_3$)
350	SO_2 twist
448	Symmetric OSO bending
471	SO_2 scissor
513	SO_2 wag
561	~ Asymmetric OSO bending in Sodium dithionate ($Na_2S_2O_6$)

668	Symmetric OSO bending in Sodium thiosulphate ($Na_2S_2O_3$)
929	SO_2 symmetric stretch
974	~ SO symmetric stretch in Sodium Sulphite (Na_2SO_3)
1005	SO_2 symmetric stretch
1030	SO_2 symmetric stretch
1054	SO_2 asymmetric stretch
1072	SO_2 asymmetric stretch
1108	Asymmetric SO stretching in Sodium thiosulphate ($Na_2S_2O_3$)
1175	Asymmetric SO stretching in Sodium thiosulphate ($Na_2S_2O_3$)

High pressure effects are investigated in quasi hydrostatic and non-hydrostatic pressure environments. In first section we have reported high pressure study on ($Na_2S_2O_4$) in a quasi-hydrostatic (100 cst silicone oil) pressure environment and in second section reported high pressure study in non-hydrostatic pressure environment. As the pressure on the sample is increased, it is observed that all vibrational modes in both environments are blue shifted.

5.3.3 High Pressure Study of Sodium Dithionite ($Na_2S_2O_4$) in Quasi-hydrostatic Pressure Environment

High pressure Raman spectra of $Na_2S_2O_4$ subjected to quasi-hydrostatic pressure conditions from 0 to 34.5 GPa is shown in Figure 5.7. Silicone oil peaks can be observed in the spectra at 499 cm^{-1}, doublet at ~699 cm^{-1} and ~720 cm^{-1} and 1421 cm^{-1}, but these peaks are not visible above 6.6 GPa. An interesting relationship was observed between the S-S stretching vibrational mode at ~261 cm^{-1} and the SO_2 asymmetric stretching vibrational mode at ~1054 cm^{-1}.

As quasi-hydrostatic pressure increases to a very low pressure of 0.3 GPa many modes show change in dω/dP. The first SO symmetric stretching mode ~1005 cm^{-1} vanishes at 3.2 GPa. S-S vibrational mode (261cm^{-1}) is observed to develop a shoulder peak at high frequency and decrease in intensity at 7.8 GPa. At same pressure of 7.8 GPa when S-S vibrational mode (261cm^{-1}) develops a shoulder peak at high frequency, SO_2 asymmetric stretch mode (1054 cm^{-1}) begins to merge with the SO_2 symmetric stretch (1030 cm^{-1}).

When the merging is complete at 12.7 GPa, the original low frequency S-S vibrational mode (261cm^{-1}) intensity continues to be reduced, but a newly generated S-S mode on the high frequency side of the original S-S vibrational mode (261cm^{-1}) continues to rise and becomes the spectrum's most intense peak. The dω/dP value for the SO_2 symmetric stretching mode (1030 cm^{-1}) at 15.8 GPa clearly indicates pressure induced changes in the molecule.

The original S-S stretching mode vanishes above 18.7 GPa, but a new S-S stretching mode on the high frequency side can be observed up to a maximum compression of 34.5 GPa. At a very low pressure of 0.3 GPa, the SO_2 asymmetric stretch mode (1072 cm^{-1}) exhibits the first change in dω/dP. Both of the modes, 1030 cm^{-1} and 1054 cm^{-1} show changes in the dω/dP value at 24.8 GPa. The deconvolution of SO_2 asymmetric stretch mode (1054 cm^{-1}) from SO_2 symmetric stretch (1030 cm^{-1}) occurs at 24.5 GPa, at the same pressure when 1030 cm^{-1} and 1054 cm^{-1} show changes in frequency variation around 24.8 GPa.

Another sign of the deconvolution is indicated by the drop in intensity of the newly formed S-S vibrational mode (261cm^{-1}) on the high frequency side at 24.5 GPa. The SO_2 asymmetric stretch mode (1054 cm^{-1}) continued to deconvolute from the SO_2 symmetric stretch (1030 cm^{-1}) up to 34.5 GPa pressure and the intensity of the newly formed S-S vibrational mode 261cm^{-1} on the high frequency side dropped in intensity. At 0.3, 7.8, and 18.7 GPa, the S-S vibrational mode (178 cm^{-1}) exhibits a change in frequency while the SO_2 wagging mode (513 cm^{-1}) exhibits a frequency change at 7.8 GPa. The SO_2 twist mode (350 cm^{-1}) and S-S vibrational mode (261 cm^{-1}) merge at 12.7 GPa and merging continues all the way up to very high pressure. At the same pressure of 12.7 GPa, SO_2 asymmetric stretch mode (1054cm^{-1}) completely merged with SO_2 symmetric stretch (1030cm^{-1}).

At 17–18 GPa, changes in dω/dP are observed in SO_2 twist (350 cm^{-1}) and SO_2 symmetric stretch (929 cm^{-1}). At 3.2 GPa, the SO_2 symmetric stretch (1005 cm^{-1}) merges with the SO_2 symmetric stretch (1030 cm^{-1}). In Figure 5.8, Raman frequency versus pressure depicts the changes by induced pressure in a quasi-hydrostatic environment.(Shah et al., 2022)

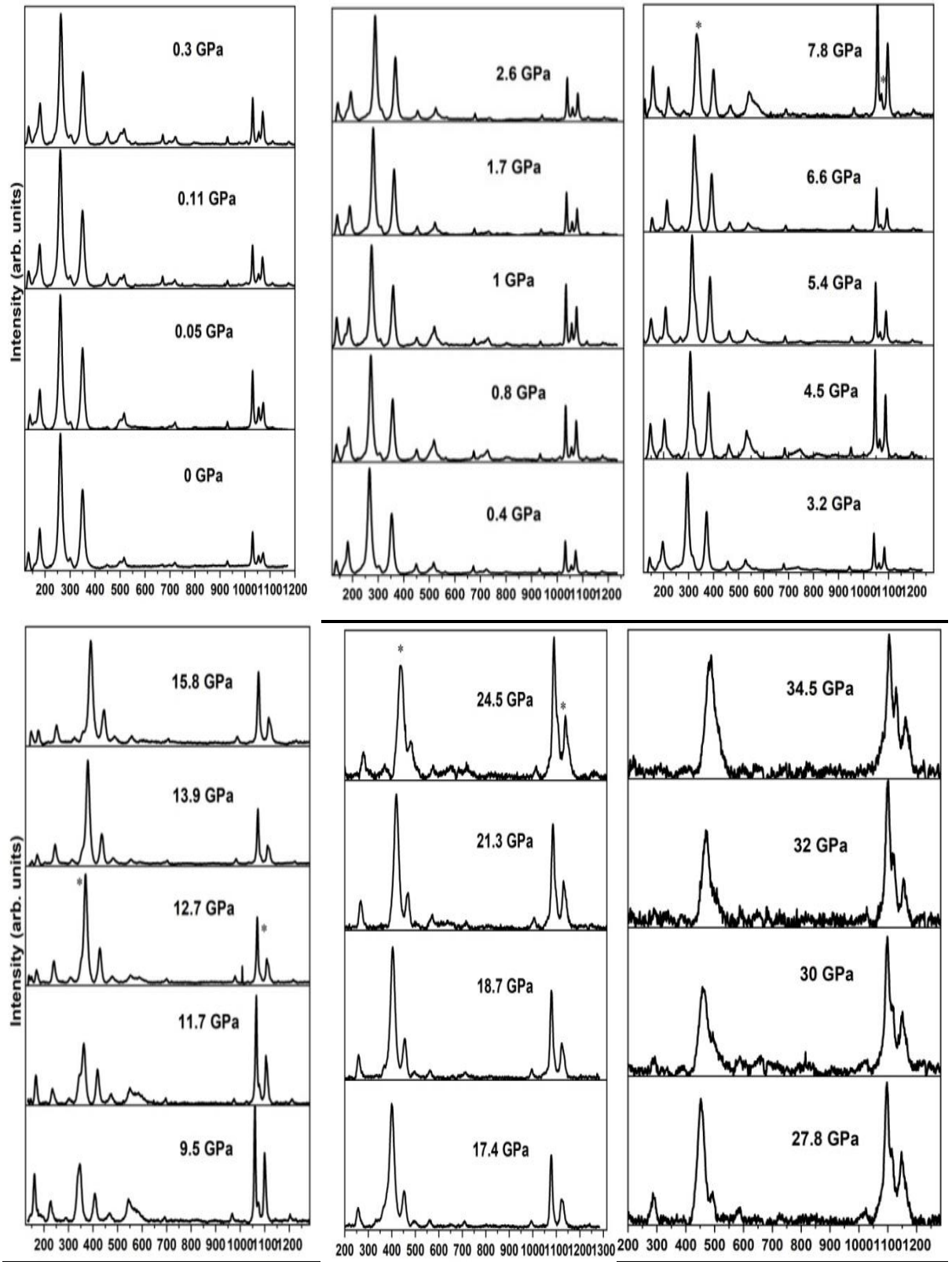

Figure 5.7: Raman spectra of Sodium dithionite ($Na_2S_2O_4$) under quasi hydrostatic pressure (0-34.5GPa).(Shah et al., 2022)

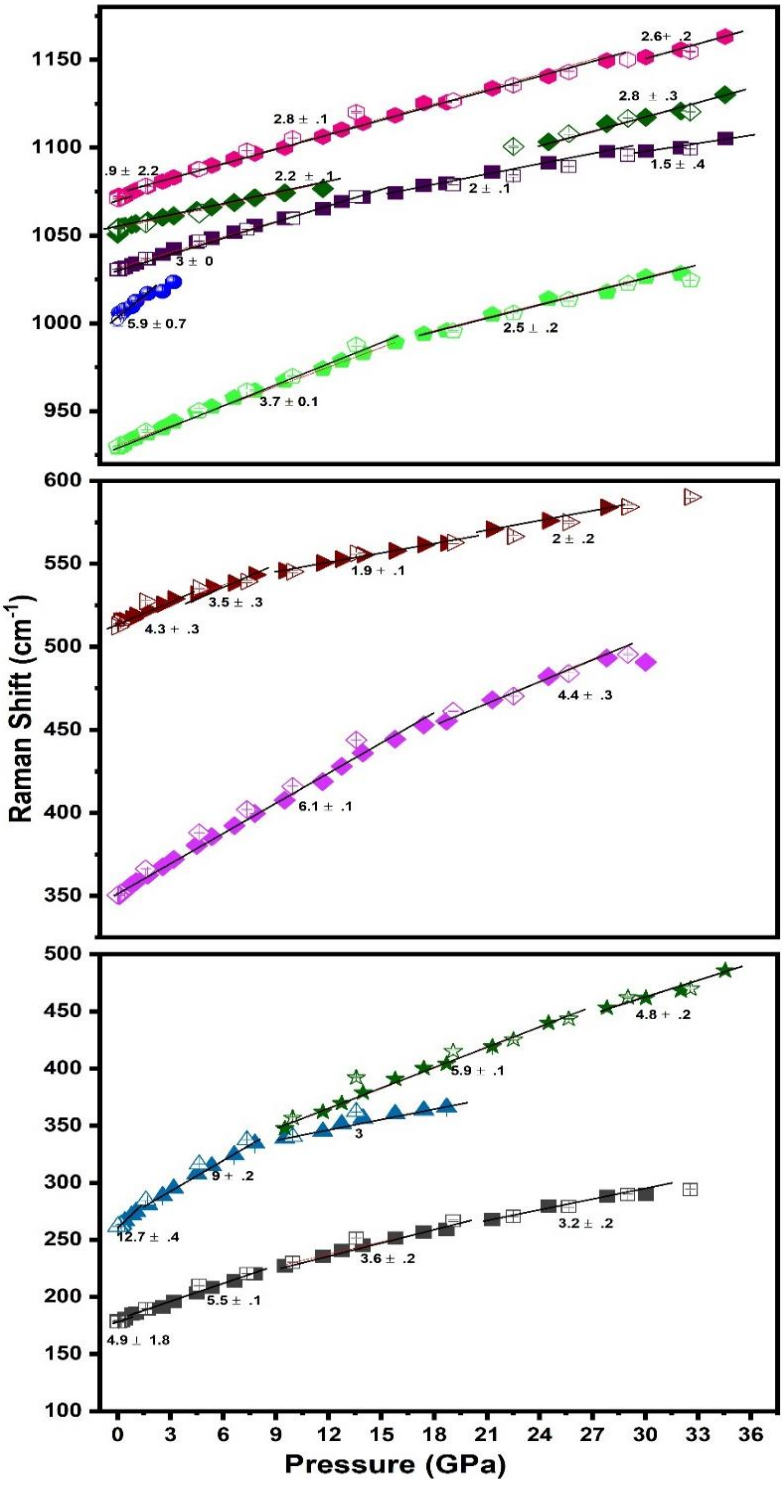

Figure 5.8: Raman modes' pressure dependency under quasi-hydrostatic pressure. The filled and open symbols represent compression and decompression, respectively.

When the sample is completely decompressed in a quasi-hydrostatic pressure environment, Raman spectra is completely reversible with respect to the peak positions, as shown in Figure 5.9. But the relative intensity of some modes doesn't recover to the same intensity as the original sample. Normalized Raman Spectra of $Na_2S_2O_4$ under quasi-hydrostatic pressure is

plotted in Figure 5.9. Where black line show Raman spectrum at lowest pressure of 0 GPa and red line show Raman spectra recorded when diamond anvil cell was fully decompressed.

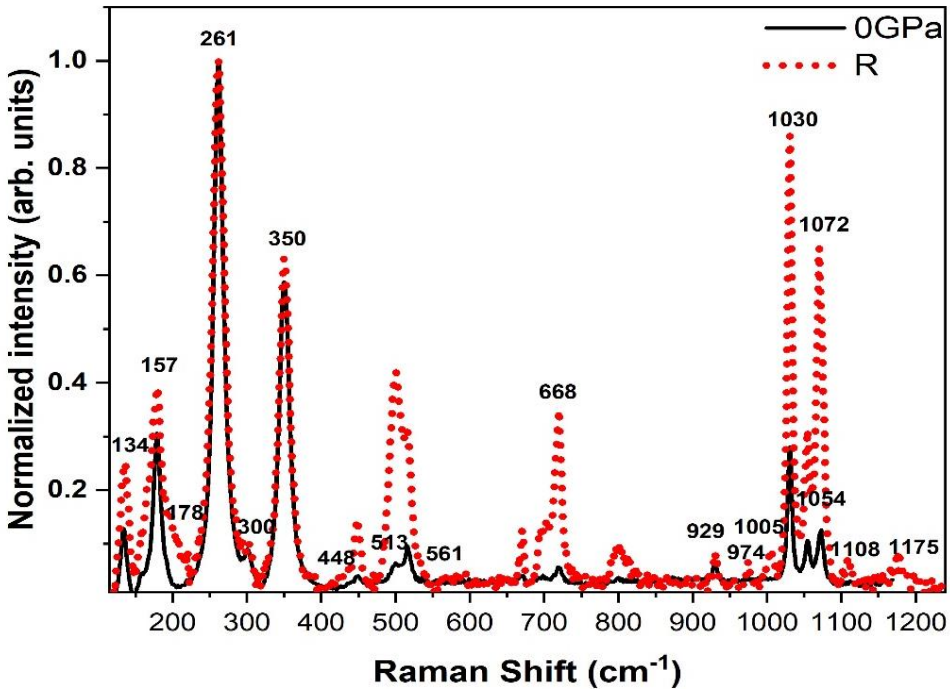

Figure 5.9: Under quasi-hydrostatic pressure, the normalized Raman spectra of $Na_2S_2O_4$ – Black (At lowest pressure-0 GPa) and Red (fully decompressed).

5.3.4 High Pressure Study of Sodium Dithionite ($Na_2S_2O_4$) in Non-hydrostatic Pressure Environment

In Figure 5.10, a high pressure study of Sodium dithionite ($Na_2S_2O_4$) in a non-hydrostatic pressure environment ranging from 0 to 30.2 GPa is depicted. On compression, all the modes were found to be blue shifted. As non-hydrostatic pressure increases to 7.8 GPa, the SO_2 asymmetric stretching mode (1054 cm^{-1}) begins to merge with the SO_2 symmetric stretching mode (1030 cm^{-1}) and was completely merged at 8.8 GPa. When the compression increases to 22.9 GPa, the SO_2 asymmetric stretch mode (1054 cm^{-1}) starts deconvoluting from the SO_2 symmetric stretch mode (1030 cm^{-1}).

At 7.8 GPa, a new mode is developed at the higher frequency side of the S-S vibrational mode (261cm^{-1}) and at the same pressure, S-S vibrational mode (178 cm^{-1}) shows a change in $d\omega/dP$. As pressure increases, the old S-S vibrational mode at lower frequency side weakens in intensity while newly developed mode at higher frequency side intensifies. The SO_2 twist mode

(350 cm^{-1}) starts to merge with the high frequency shoulder of the S-S vibrational mode (261 cm^{-1}) at 8.8 GPa and at 26.4 GPa merging of both modes (350 cm^{-1} and 261cm^{-1}) is completed. Around 11 GPa, SO_2 wag mode (513 cm^{-1}) shows a change in dω/dP. Both SO_2 symmetric stretch (929 cm^{-1}) and SO_2 asymmetric stretch mode (1072 cm^{-1}) show a change in dω/dP first around 13 GPa and then at 22.9 GPa. At a low pressure of 1.6 GPa, the SO_2 symmetric stretch (1005 cm^{-1}) merges with the SO_2 symmetric stretch (1030 cm^{-1}). Figure 5.11 depicts the Raman frequency versus pressure changes when non-hydrostatic pressure is induced on the sample. Figure 5.12 shows that all the peaks in the spectra show red shift during decompression and are completely reversible in terms of peak positions and peak intensities.(Shah et al., 2022)

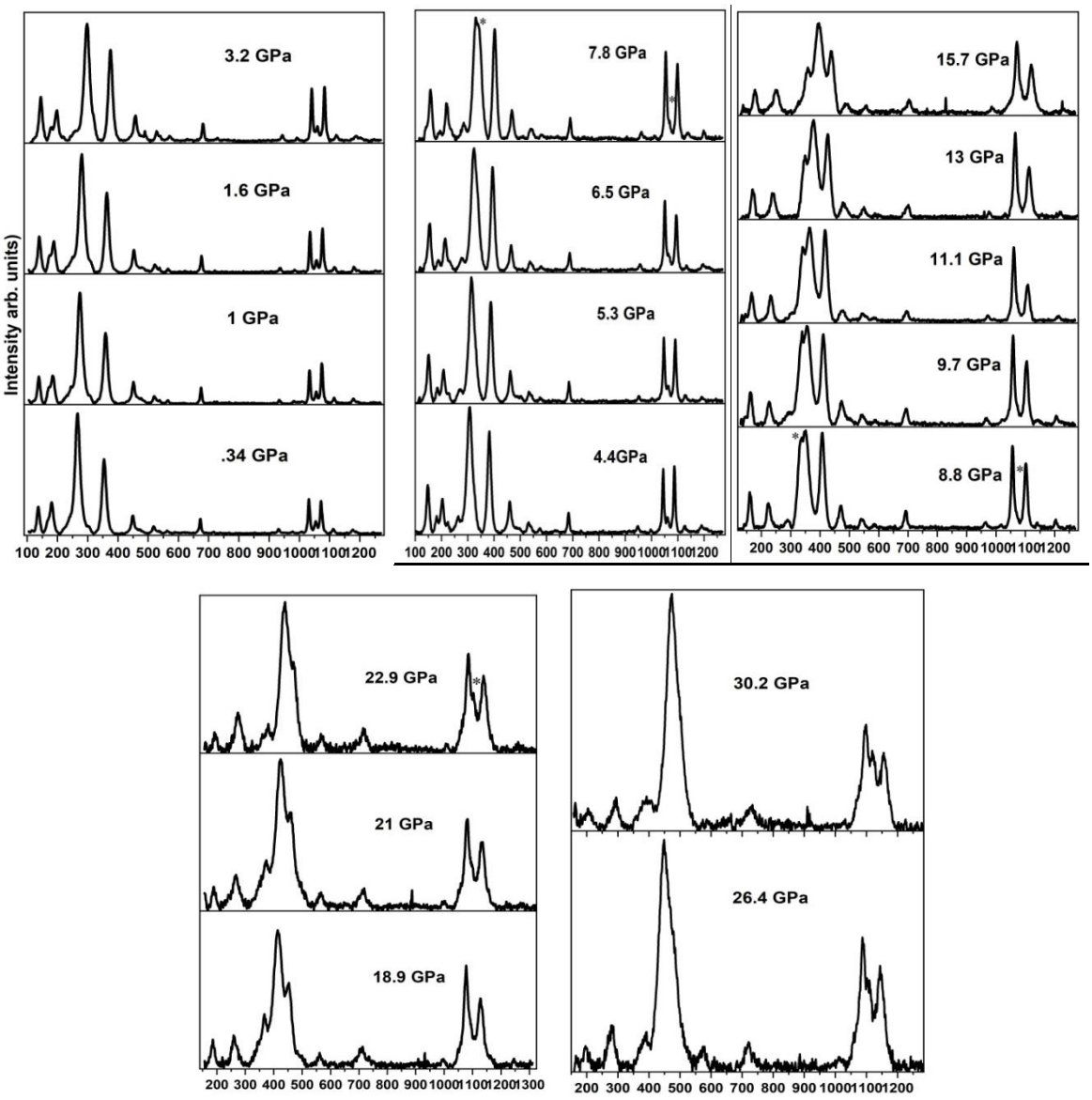

Figure 5.10: Raman spectra of Sodium dithionite ($Na_2S_2O_4$) under non-hydrostatic pressure (0-30.2 GPa).(Shah et al., 2022)

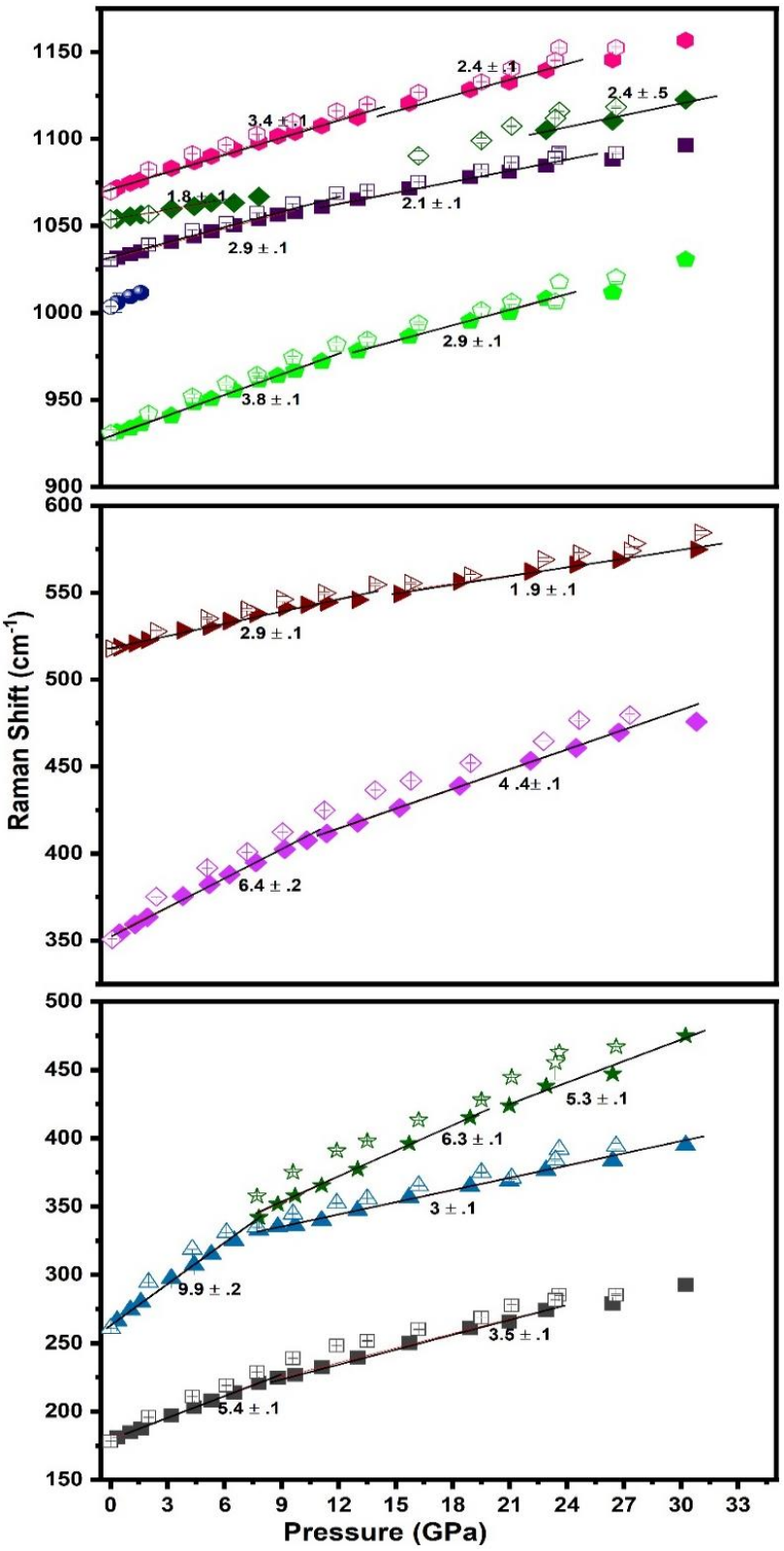

Figure 5.11: Raman modes' pressure dependency under non-hydrostatic pressure. The filled and open symbols represent compression and decompression, respectively.

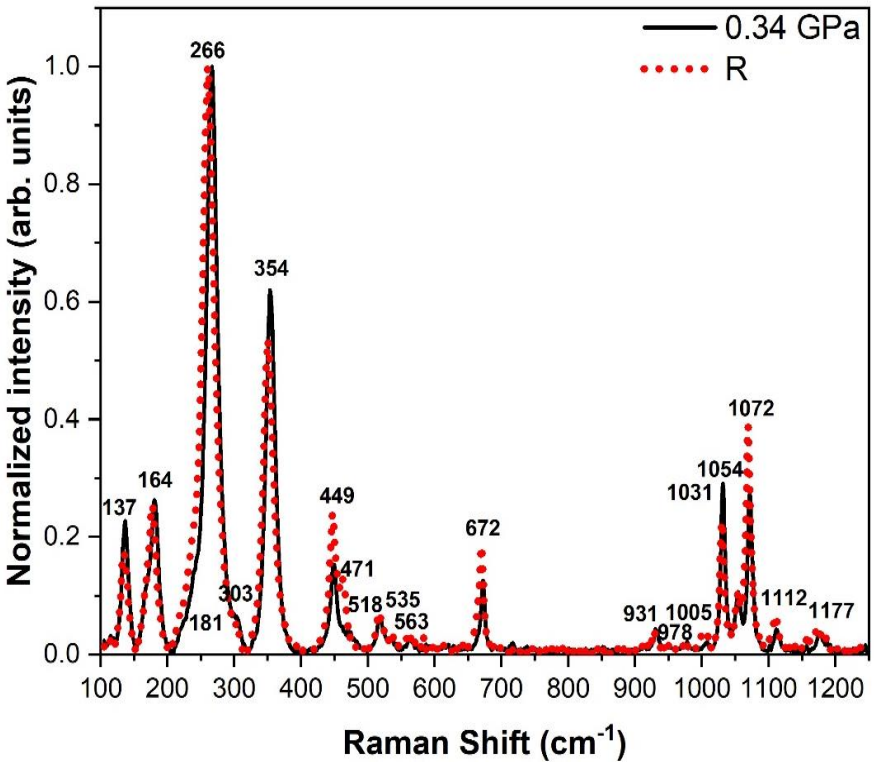

Figure 5.12: Under non-hydrostatic pressure, the normalized Raman spectra of $Na_2S_2O_4$ – Black (At lowest pressure-0 .34 GPa) and Red (fully decompressed).

In summary, S-S vibrational mode (261 cm^{-1}) develops a new mode on the higher frequency side of the original S-S vibrational mode (261cm^{-1}) in a quasi-hydrostatic pressure environment, and both modes exhibit intensity fluctuation during compression. Above 18.7 GPa, the original S-S vibrational mode vanishes, however the newly formed S-S vibrational mode exhibits intensity fluctuation. It has been observed that the newly formed S-S vibrational mode is observed up to maximum compression of 34.5 GPa.

In a non-hydrostatic pressure environment, a new mode on the higher frequency side of S-S vibrational mode (261 cm^{-1}) is developed. The original S-S vibrational mode remains present as a weak shoulder and does not disappear up to a maximum compression of 30.2 GPa. The newly formed S-S vibrational mode does not exhibit intensity fluctuation.

Thus, the development of the newly formed high frequency shoulder in the S-S vibrational mode and variation of intensity is associated with the merging and unmerging of the SO_2 asymmetric stretching vibration (1054 cm^{-1}) with the SO_2 symmetric stretching mode (1030 cm^{-1}).

In the Raman spectra of $Na_2S_2O_4$, changes were observed at pressures of ~ 0.3 GPa, ~ 3.2 GPa, ~7.8 GPa, and ~18.7 GPa. These pressure values are similar to the pressure values that were observed in high pressure studies of SO_2 (Song et al., 2005; Swanson et al., 1982; H. Zhang et

al., 2020)According to studies (Song et al., 2005; H. Zhang et al., 2020), at 0.3 GPa, SO_2 changes from the Orthorhombic I phase to the disordered phase. Around 2.5 GPa, it undergoes a first order phase transition into the crystalline Orthorhombic II phase, which is stable till 17.5 GPa. In the Raman spectra of SO_2, major changes were observed beyond 17.5 GPa, which were related to enhanced interactions between SO_2 molecules. (Song et al., 2005) It transforms from molecular amorphous to polymeric amorphous form at a pressure of around 26 GPa, showing the intertwining polymeric chains of 3-coordinated Sulphur atoms via Oxygen atoms. (H. Zhang et al., 2020)

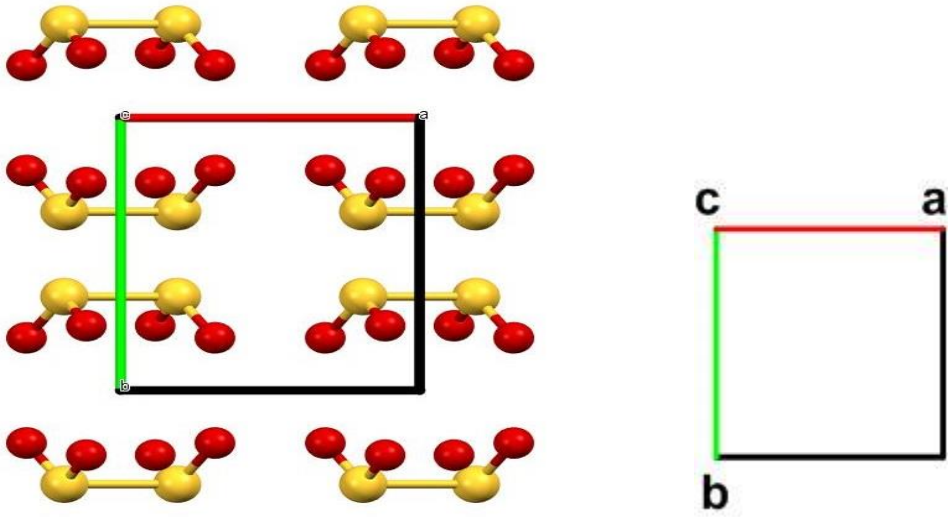

Figure 5.13: Structure of crystalline sodium dithionite ($Na_2S_2O_4$)

We propose that the majority of the vibrational modes in quasi-hydrostatic pressure (uniform stress) are affected at pressures as low as 0.3 GPa, and this pressure value matches the first phase transition observed in SO_2. The investigation at quasi-hydrostatic pressure demonstrates that SO_2 vibrations are significantly influenced by S-S bond polarizability and, therefore, its intensity.

At ambient pressure, the distance between the oxygen atoms of one dithionite ion and the sulphur atoms of the backwardly facing dithionite ion is 3.343 Å in the ac plane as shown in Figure 5.13. We believe that the van der Waals gap might be reduced due to the pressure and orient the former dithionite ion's SO bonds toward the sulphur atom of the latter, forming a staggered or gauche conformation, exhibiting significant interaction between the nearby $Na_2S_2O_4$ units. This might be the reason of the SO_2 wagging mode's slow blue shift. At 7.8 GPa, a new peak starts to appear on the high frequency regions of S-S bond (261cm-1), whereas the original S-S bond entirely breaks at 18.7 GPa. In high pressure study significant variations were observed in the structure of SO_2 around 17.5 GPa. (Song et al., 2005; H. Zhang et al.,

2020). However, all of the Raman modes in our investigation are much like the ambient structure. As a result, we tend to hypothesise that at a pressure of 7.8 GPa, new S-S bonds get formed with the sulphur atoms of neighbouring chains. For few pressures, the old and new S-S bonds coexist, but the original S-S bonds eventually break at a pressure of around 18.7 GPa. That gives $Na_2S_2O_4$ a new structure, and it probably changes the orientation of the molecules in the unit cell. Some hysteresis persists after decompression, as all vibrational modes retain their positions, although they don't regain their relative intensities in comparison to their original spectra.

However, in a non-hydrostatic pressure environment, the original S-S stretching mode splits at high frequency shoulder. We believe that the van der Waals gap might be reduced in non-hydrostatic pressure environment due to a shear stress component may cause sliding of the 'ac' plane containing the S-S bonds against the neighbouring 'ac' plane. (Figure 5.13) Due to this slipping, two sulphur atoms of the backward-facing dithionite ions get close to each other and form a new S-S bond and, the original dithionite ion's S-S bond weakens. Formation of new S-S bond at high frequency side is similar to the quasi-hydrostatic pressure environment.

The vibrational mode corresponding to the newly formed S-S bond (high frequency mode) becomes more noticeable with an increase in pressure and the original S-S bond (low frequency mode) weakens. The molecules regain their individual structures after decompression, with no hysteresis.

It is clearly evident from Figures 5.8 and 5.11 that the original and newly formed S-S bonds have different slopes of ω against pressure. It shows a difference in behaviour under pressure. It could be attractive to correlate the emergence of a new S-S bond around 7.8 GPa and its subsequent extinction around 18.7 GPa (during quasi-hydrostatic pressure run) or weakening with pressure (during non-hydrostatic pressure run) with the sulphur atoms' tendency to transform into 3-coordinated atoms, which can help to form polymeric chains or clusters at high pressure. Despite the fact that our data shows that SO_2 units are driving high pressure changes, it may not be possible to develop polymeric chains or clusters since it would show substantial changes in Raman spectra. The Raman spectra of $Na_2S_2O_4$ do not show significant changes at high pressures to that extent. We hypothesise that $Na_2S_2O_4$ molecules form a new structure at pressures around 7.8 GPa with different orientation of $Na_2S_2O_4$ molecules, enabled by reduction of van der Waals distance between ac planes and formation of new S-S bonds among neighbouring chains. The phase transition is completed for quasi-hydrostatic pressure,

as the original S-S stretching mode disappears in Raman spectra, while for non-hydrostatic pressure, the original S-S stretching mode doesn't completely disappear till the maximum pressure of 30.2 GPa, and occurs with residual effects. In quasi-hydrostatic pressure environment, one more difference is observed. The intensity of the S-S stretching mode fluctuates with the merging and unmerging of the S-O symmetric and antisymmetric stretching modes. In both pressure environments during decompression, similar splits in the S-S vibration peak were observed. On decompression, the reversible Raman spectrum strongly suggests a coordinated network as the most probable reason, in our opinion, in the formation of new S-S bonds in neighbouring chains.

5.4 Conclusion

In our work, we performed a systematic high pressure study on $Na_2S_2O_4$ and studied it under quasi-hydrostatic and non-hydrostatic pressure environments. High pressure solid state reactions between sodium dithionite and ketones showed a decrease in the intensity of the vibrational mode corresponding to the carbonyl bond, which indicates the formation of a chiral center of a particular carbon atom attached to ketones. The dynamics of sodium dithionite under extreme pressure shows that sodium dithionite ($Na_2S_2O_4$) can act like a chirality inducing agent. This study shows that $Na_2S_2O_4$ acts as two separate units of $(SO_2)^-$ when it is under high pressure in its solid state. The latter feature is comparable to aqueous solutions of $Na_2S_2O_4$, which is an environmental pollutant that has been extensively studied as a reducing agent. The asymmetric stretching mode (1054 cm^{-1}) merges with SO_2 symmetric stretch mode (1030 cm^{-1}) at 7.8 GPa in both pressure environments and deconvolutes at higher pressures. In a quasi-hydrostatic pressure environment, the merging of these SO_2 stretching modes led to the development of a new blue shifted S-S stretching mode and the breaking of the original S-S bond (261 cm^{-1}). While in a non-hydrostatic pressure environment, a new blue shifted S-S stretching mode is developed but the original S-S bond (261 cm^{-1}) intensity is reduced. We propose that in the case of quasi-hydrostatic pressure, a new structure is formed with a different orientation of $Na_2S_2O_4$ molecules in the unit cell, while in the case of non-hydrostatic pressure, linear chains are formed along the c axis. When the sample was decompressed in a non-hydrostatic pressure environment, residual effects provided a remarkable memory effect to the lattice, whereas some hysteresis was observed as the old S-S bond broke in a quasi-hydrostatic

pressure environment. Our findings can be proven very useful by providing a novel reversible approach to understand the S-S bond's reactivity, a thrust area in biological sciences.